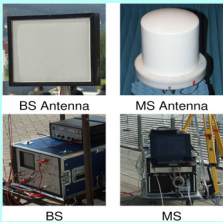


## Channel characterization and modeling for wireless communication systems

- Comparison of directional channel measurement and ray-tracing simulation in street microcell
- Application of radar cross section in ray-tracing for prediction of microcell propagation channels
- Frequency characteristic of propagation loss through foliage
- Spatio-temporal multipath clustering of wideband MIMO channel at the mobile station
- Scalable MIMO channel sounder architecture
- Performance evaluation of user terminal array antenna system
- Body area network (BAN) channel measurement and modeling
- Polarization properties of double directional channel



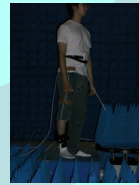
Channel sounding measurement

## Other topics

- UWB delay estimation
- Spherical harmonics modeling of directional channel
- Evaluation of EMC anechoic chamber

## Cognitive Radio and Software Defined Radio

- Performance analysis of cyclic detectors of OFDM signals
- Implementation issues of spectrum sensing in cognitive radio
- Spectrum sensing prototype implementation for ISDB-T signal
- Evaluation of open source software defined radio platform using GNURadio and USRP (universal software radio peripherals)



BAN channel measurement



GNURadio Peripherals

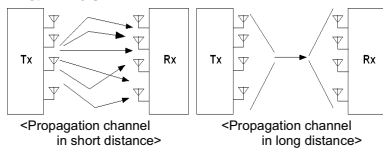
## Development of Scalable MIMO Channel Sounder Architecture for Microcell Environment

Tomoshige KAN<sup>Ⓜ</sup> · Jun-ichi TAKADA<sup>Ⓜ</sup> · Ryuhei FUNADA<sup>∞</sup> · Hiroshi HARADA<sup>∞</sup>

<sup>Ⓜ</sup> Takada Laboratory    <sup>∞</sup> Mobile Communications Research Group    <sup>∞</sup> Tokyo Institute of Technology  
<sup>∞</sup> National Institute of Information and Communications Technology

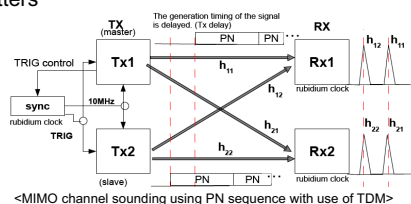
### 1 Introduction

- Requirements of 4G systems include high-capacity and high-speed (100Mbps with high mobility).
- MIMO (Multi Input Multi Output) systems have great advantages for realization of the high-speed and high-capacity.
- In Macrocell environment, MIMO system can utilize different techniques depending on the distance between Tx & Rx as
  - Short distance: High-speed communication by MIMO multiplexing transmission
  - Long distance : Keep communication quality by MIMO Diversity
- We aim at characterizing the multi-cell MIMO channel in order to evaluate system-level performance more properly.
- We developed a scalable sounder architecture with multiple SISO systems that can analyze a path loss and a delay profile characteristic used by PN sequence.



### 2 Theory of Measurement of MIMO System Using PN Sequence with The Use of TDM

- Synchronization between transmitters are taken to control the timing of the transmitted signal at each branch in TDM (time division multiplexing) manner.
- MIMO channel information can be obtained by correlation at each Rx.



### 3 Measurement System Specifications

Center frequency	3.35GHz
Band width	80 MHz
Transmission power	1mW(0dBm) (10W(40dBm) with PA)
Transmission signal	2 <sup>15</sup> -1~2 <sup>15</sup> -1PN sequences
Modulation	BPSK
chip rate	40 Mchip/s
Sampling rate	160 Msample/s (with 4oversampling)
Number of antenna	Tx=2, Rx=2
Measurement data acquisition	Real time, Every 1, 10, 100ms(2 <sup>15</sup> -1 ~ 2 <sup>14</sup> -1 PN) Every 100ms(2 <sup>15</sup> -1 ~ 2 <sup>14</sup> -1PN)
Tx delay	arbitrarily set up

### 4 Features of Scalable MIMO Measurement System

- TDM is implemented in control transmit timing.
- Continuous channel measurement is possible.
- It is easy to extend the branches by synchronization between transmitters and control of transmission timing of PN signal at each branch.
- Each transmitter transmits the PN signal at different timing.  
→ Time difference should be determined longer than maximum excess delay.
- Synchronization between Tx and Rx is not considered because absolute delay is not necessary.

### 5 Parameters of Propagation Characteristic

- Characteristic of path loss
- Measurement of received power
- Characteristic of delay profile
- Correlation of received signal at Rx
- Correlation between MIMO channels  
By synchronizing between channels, the correlation can be obtained
- Doppler power spectrum, Delay spread, shadowing etc. can be calculated.

# Spatio-temporal Multipath Clustering of an Estimated Wideband MIMO Channel at the Mobile Station

Lawrence MATERUM <sup>◇</sup> · Jun-ichi TAKADA <sup>◇</sup> · Ichirou IDA <sup>∞</sup> · Yasuyuki OISHI <sup>∞</sup>

<sup>◇</sup> Takada Laboratory <sup>∞</sup> Mobile Communications Research Group <sup>∞</sup> Tokyo Institute of Technology <sup>∞</sup> Fujitsu Limited

### 1 Framework

Microcell Site Survey & Planning for Measurement Campaign → Channel Estimation & Parameter Estimation → Middle Ground Multipath Clustering → Nonblind Multipath Clustering → Blind Multipath Clustering → Number of Multipath Clusters Adapted to Application → Global Optimization (Simulated Annealing) → Local Optimization (Scatterer Clustering)

MIMO Channel Analysis and Modeling (for scattered multipath)

We would like to thank NICT Japan for supporting this research

### 2 Goals

- Overall Goal: to know the multipath cluster behavior
- Specific Goal: to identify multipath clusters in a better way
- Motivation: to take advantage of cellular MIMO systems benefits

### 3 Channel

Environment: small urban macrocell  
BS Height: ~85 m  
MS Height: ~1.80 m  
BS-MS Separation: ~230 to 400 m  
Structure Type: residential & industrial  
Measurement Route: Kawasaki City, Japan  
MS movement: slowly walking pace

### 4 Sounder

BS Tx signal: wideband multitone  
Carrier frequency: 4.5 GHz  
Bandwidth: 120 MHz  
Patch elements: V & H pol.  
BS antenna: 2x4x2 URA  
MS antenna: 2x24x2 UCA  
Max. path delay: 3.2 μs  
Make: Medav-RUSK-Fujitsu

### 5 Double-Directional Max. Likelihood Channel Parameter Estimation

$$\mathbf{h}(\tau, \phi^{AoD}, \phi^{AoA}, \theta^{AoD}, \theta^{AoA}) = \sum_{i=1}^L \begin{bmatrix} \gamma_{VV} & \gamma_{VH} \\ \gamma_{HV} & \gamma_{HH} \end{bmatrix} \delta(\tau - \tau_i) \delta(\phi^{AoD} - \phi_i^{AoD}) \delta(\phi^{AoA} - \phi_i^{AoA}) \delta(\theta^{AoD} - \theta_i^{AoD}) \delta(\theta^{AoA} - \theta_i^{AoA})$$

### 6 Midway Approach

**Blind Clustering** (i.e. automatic or nonvisual)

- complicated real-world clusters
- mathematically tractable
- number-based
- 'better' number processor

**Nonblind Clustering** (i.e. manual or visual)

- unwieldy & subjective
- physically trackable
- object-based
- 'better' object processor

### 7 Factors Considered

Factor	Possible Quantification	Gives an answer to:
Similarity/dissimilarity measure	Multidimensional distance, probability density function, ...	How near/far are multipaths from each other?
Significance measure	shape, size, power, mutual information, target application performance ...	Which multipaths are considered?
Validation measure	clustering validity index, physics, scatterers, ...	How are the identified clusters validated?

Nonblind clustering validation criteria:

- Within-processing limitations
- Non-overlapping in delay
- Scatterer existence

### 8 Clustering Problem

NP-hard combinatorial minimization

$$\text{minimize } \sum_{k=1}^K \sum_{i \in C_k} V_{ik} d(\mathbf{X}_i, \mu_k)$$

subject to  $\sum_{k=1}^K V_{ik} = 1, V_{ik} \in \{0, 1\}$

$d(\cdot)$ : multipath-distance measure  
 $\mathbf{X}_i$ :  $[\tau_i, x_i^{AoD}, y_i^{AoD}, z_i^{AoD}, \phi_i^{AoA}, \theta_i^{AoA}, \phi_i^{AoD}, \theta_i^{AoD}]$   
 $\mu_k$ :  $k^{\text{th}}$  cluster centroid  
 $K, L$ : no. of multipath clusters; paths  
 $V_{ik}$ :  $\mathbf{X}_i$  assignment indicator to  $C_k$

### 9 Local Optimization

$$\min_{\{C_k\}_{k=1}^K} \left[ \sum_{k=1}^K \sum_{i \in C_k} d(\mathbf{X}_i, \mu_k) \right]$$

Cluster assignments updated until convergence

### 10 Global Optimization

- Simulated Annealing: well-known globally stochastic optimization strategy
- A form of the Metropolis-Hastings algorithm

### 11 No. of Clusters

- A priori knowledge is not available
- Clustering Validity Index: tells the best grouping
- Criteria: compactness & separation
- Optimizing in nature

### 12 Cluster Mechanisms

Clustering Validity Indices

- Silhouette index:  $K_{SI} = \arg \max_K \left\{ \frac{1}{K} \sum_{i \in C_k} \left( \frac{1}{|C_k|} \sum_{j \in C_k, j \neq i} s_{ik} \right) \right\}$
- Davies-Bouldin index:  $K_{DB} = \arg \min_K \left\{ \frac{1}{K} \sum_{k=1}^K \left( \arg \max_{l \neq k} \left\{ \frac{s_{kl} + s_{lk}}{d(\mu_k, \mu_l)} \right\} \right) \right\}$
- Calinski-Harabasz index:  $K_{CH} = \arg \max_K \left\{ \frac{\text{Trace}(\mathbf{B}(K-1))}{\text{Trace}(\mathbf{W})/(L-K)} \right\}$
- Kim-Parks index:  $K_{KP} = \arg \min_K \left\{ \left( \frac{1}{K} \sum_{k=1}^K S_k \right) + \frac{K}{\arg \min_{i \in C_k} \{d(\mu_i, \mu_j)\}} \right\}$
- Dynamic index:  $K_{DI} = \arg \min_K \left\{ \frac{\arg \max_{i \in C_k} \{d(\mu_i, \mu_j)\}}{\arg \min_{i \in C_k} \{d(\mu_i, \mu_j)\}} + \frac{\sum_{i \in C_k} \text{var}(\mathbf{X}_i)}{\sum_{i \in C_k} \text{var}(\mathbf{X}_i)} \right\}$

Average Rank Aggregation

- It is not straightforward to normalize these clustering validity indices,  $s_r(K)$
- Scoring by statistical rank,  $sr(s_r)$
- Does not depend on weighting

### 13 MS Results

Cluster Scatterer	Overall [%]
Metal	35.3
Concrete	30.4
Asphalt	16.7
Brick	9.3
Mixed	8.3

### 14 PSD Examples

### 15 Cluster Correlation

Parameter 1	Parameter 2	Corr. Coef.
Delay $\sigma$	Azimuth AoD $\sigma$	0.65
Fading factor	CPR	0.53
Power	CPR	-0.41
No. of clusters	Fading factor	-0.35

# Application of Radar Cross Section in Ray Tracing for Prediction of Microcell Propagation Channels

Yukiko KISHIKI <sup>◇</sup> · Jun-ichi TAKADA <sup>◇</sup>

<sup>◇</sup> Takada Laboratory <sup>∞</sup> Mobile Communications Research Group <sup>∞</sup> Tokyo Institute of Technology <sup>∞</sup> Kozo Keikaku Engineering Inc., Japan

This work discusses the problems of the geometrical optics (GO) approximation and investigates the applicability of GO in a microcell environment. In addition, the complex radar cross section (RCS) is introduced to apply GO to the areas where it is not directly applicable. Finally the ray tracing simulator has been expanded to handle the RCS. The improvement of the simulation accuracy is also validated by comparing with measured results.

### Step 1

**Definition of the small scattering object**  
The region where the Geometrical Optics (GO) can be applicable is surveyed.

### Step 2

**Introduction of complex Radar Cross Section (RCS)**  
The coefficients of scattering modeled by RCS is introduced.

### Step 3

**Application of complex RCS to ray tracing calculation.**

### Results

- The path loss of the conventional technique deviates from measurement at long distances.
- The path loss of proposed technique is closer to the measurement data.

### Step 1

Comparison between Physical Optics (PO) & Stationary Phase method (SP).

- PO — Specular Reflection  
⇒ True diffraction: PO diffraction
- Edge Diffraction  
⇒ GO diffraction

### Step 2

For the range where GO fails

Complex Radar Cross Section

$$\sigma_{cs} = \frac{-jkLW}{\sqrt{\pi(1+Z/\eta)}} (Z/\eta \hat{n} \cdot \hat{h}_r \times \hat{e}_i + \hat{n} \cdot \hat{e}_r \times \hat{h}_i) \times \frac{\sin[1/2kL \cdot (\hat{i}-\hat{s})] \sin[1/2kW \cdot (\hat{i}-\hat{s})]}{1/2kL \cdot (\hat{i}-\hat{s})} \frac{\sin[1/2kL \cdot (\hat{i}-\hat{s})]}{1/2kW \cdot (\hat{i}-\hat{s})} e^{jkR_0 \cdot (\hat{i}-\hat{s})}$$

Complex RCS is introduced in order to calculate the coherent scattering from multiple objects

### Step 3

Implemented scattering mechanisms

- Specular Reflection
- Transmission
- Diffraction
- Scattering modeled by RCS

Scattering path modeled by RCS

Electric field's formula

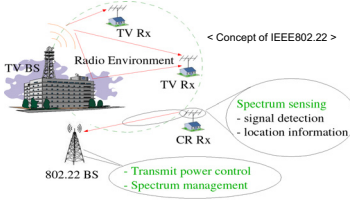
$$E_i = \frac{\lambda E_t}{4\pi s_{i,1}} \mathbf{g}_t(\hat{i}) \cdot \hat{R}_t \cdot \hat{T}_t \cdot \sqrt{\sigma_{cs}} \cdot \mathbf{g}_r(\hat{i}) \frac{e^{-jk s_{i,2}}}{\sqrt{4\pi s_{i,2}}}$$

Distance between Tx - Scattering by RCS:  $s_{i,1}$   
Reflection Coefficient:  $\hat{R}_t$   
Transmission Coefficient:  $\hat{T}_t$   
Antenna gain:  $\mathbf{g}_t(\hat{i})$   
RCS:  $\sqrt{\sigma_{cs}}$   
Distance between scattering by RCS - Rx:  $s_{i,2}$

- The 1<sup>st</sup> Fresnel zone is made between Tx & mirror point of Rx.
- The diffraction & the specular reflection paths within the 1<sup>st</sup> Fresnel zone are deleted.
- Within the 1<sup>st</sup> Fresnel zone, scattering from the surfaces are coherently summed up.

## Cognitive Radio & Spectrum Sensing

- As a growing interest in the cognitive radio technology has been taken based on the idea of opportunistic spectrum use, the spectrum sensing is more and more important to ensure that cognitive radios would not interfere with primary user system. Key challenge of spectrum sensing is the detection of weak signals with almost zero misdetection rates.
- IEEE802.22 is a challenge to utilize TV broadcasting band for unlicensed cognitive radio system.



## Study on Spectrum Sensing

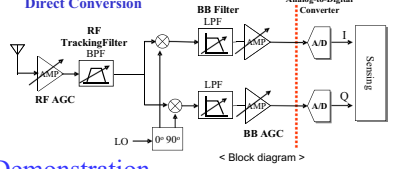
This work aims at

- Sensing algorithm development and performance analysis
  - Energy detector, Cyclostationary detector
- Study on sensing system with diversity combining and network cooperation
  - Multiple cyclic frequency
  - Multiple sensors
  - Multiple antenna
- Study on signal processing architecture
  - Parallel sensing scheme using polyphase filterbank
- Prototype implementation and investigation of practical issue
  - Practical evaluation with real signal and hardware
  - Evaluation of hardware imperfection

## Spectrum Sensing Evaluation System

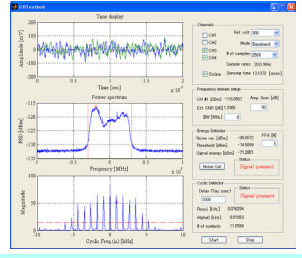
**> Feature**

- Configured by some off-the-shelf components and digital signal processing unit (DSPU)
- RF receiver module includes direct-conversion TV tuner LSI (MAX3580). It features dynamic gain control of around 80 dB and a typical noise figure of 4.7~6.5 dB.
- The signal processing part incorporates 16 channels of 14-bit ADCs and DACs, and high density FPGAs for array signal processing.
- The maximum storage : 8 mega words per channel.



**> Demonstration**

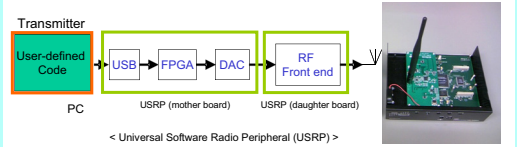
- MALAB based realtime visualization of energy and cyclostationary detector
- Snapshot of ISDB-T Mode-3 (CH25@545MHz, Nihon TV)



## GNURadio Opensource Platform

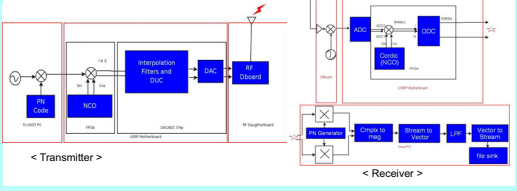
**> What is GNURadio and USRP**

- GNU Radio is a free software development toolkit that provides the signal processing runtime and processing blocks to implement software radios using readily-available, low-cost external RF hardware and commodity processors.
- Universal Software Radio Peripheral is a general purpose motherboard which hosts a wide range of RF daughter boards which can be used with the signal processing blocks found in the GNU Radio software package to give access to the radio frequency spectrum.



## > Channel sounder implementation

- An 2.4-2.5 GHz, 4.9-5.9 GHz indoor channel sounder based on PN sequence correlation is being studied as one of the GNU radio -USRP based potential applications.
- GNURadio provides very low cost and scalable MIMO channel sounder implementation



# Implementation Issues of Spectrum Sensing for Cognitive Radio System

## Objective

- To analyze the effect of practical detection issues on detection performance of energy detector:
  - Effect of quantization
  - Effect of noise uncertainty

## Effect of Quantization

**> Motivation**

- Detection performance depends on quantized samples, not on ideal samples
- What difference does quantization add to detection performance?

**> Energy Detector**

Primary signal  $H_0: x[n] = w[n]$

Channel is vacant  $H_1: x[n] = h[n] \cdot s[n] + w[n]$

Channel is being used

No. of samples  $n = 1, 2, \dots, N$

Received signal

Additive white Gaussian noise (Receiver noise)

Characteristic of the propagation channel

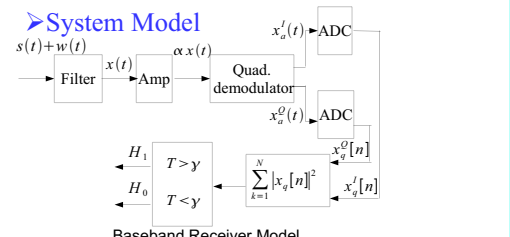
Decision statistic for energy detector  $T = \sum_{n=1}^N x[n] x^*[n]$

$H_1$  is true if  $T \geq \gamma$  (threshold that can be determined for a given  $P_{fa}$ )

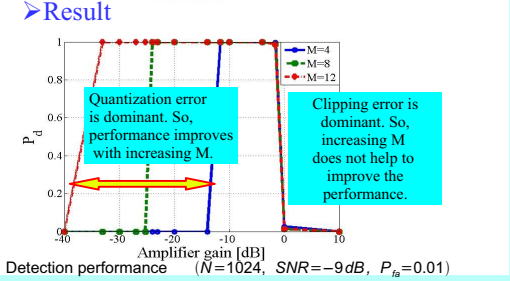
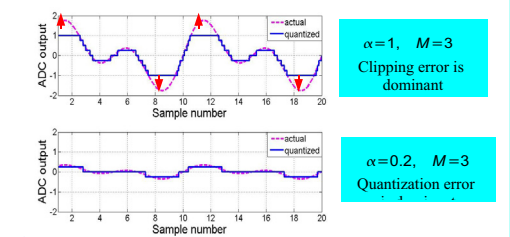
$H_0$  is true if  $T < \gamma$

Noise variance  $\sigma_w^2$

$Q(x) = \frac{1}{\sqrt{2\pi}} \int_x^{\infty} \exp(-\frac{t^2}{2}) dt$



\*Let us assume that the input to the ADC is normalized and its full scale range (FSR) is  $\pm 1$



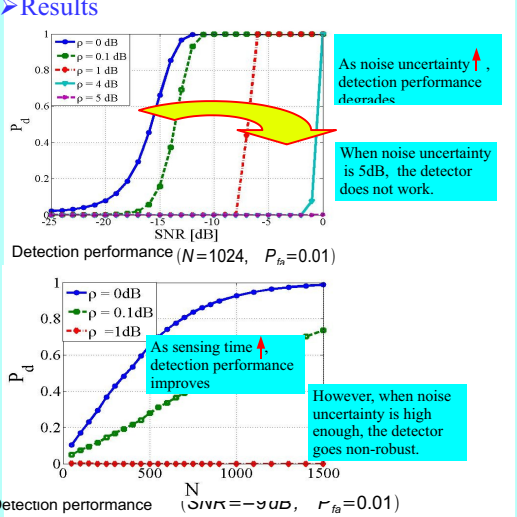
## Effect of Noise Uncertainty

**> Motivation**

- General assumptions: noise AWGN with exactly known variance. In reality: neither perfectly Gaussian nor its variance is exactly not known.
- Let the noise process  $w[n]$  has any distribution  $W$  from noise uncertainty set
- Distributional uncertainty of noise for ED:  $\sigma_w^2 \in [(\sigma_n^2 - \rho)_{dB}, (\sigma_n^2 + \rho)_{dB}]$  a parameter that quantifies the size of noise uncertainty,  $\rho > 0$

actual noise variance  $\sigma_w^2$

nominal noise variance  $\sigma_n^2$



## Abstract

Wireless body area network (BAN) is a promising part of future wireless communications. At present, wireless BAN standardization is proceeding in IEEE802.15 Task Group 6 (BAN). It is developing a communication standard optimized for low power devices and operation on, in or around the human body (but not limited to humans) to serve a variety of applications including medical, consumer electronics / personal entertainment and other. The major difference between BAN and other wireless network is to treat human body itself as the main part of the propagation channel. Antenna effect cannot be separated from the propagation channel. This work aims at dynamic wireless BAN channel measurement and modeling through detail analysis of the interaction between antenna and human body. This poster describes the measurement campaign using a human specimen and investigates the characteristics of body surface propagation in dynamic conditions.

## What is BAN

- Definition
  - Short range wireless communication in the vicinity of, or inside, a human body
  - Smaller area than PAN (Personal Area Network)
- Applications
  - Medical / Healthcare
    - Implantable medical devices
    - Swallowable devices
  - Wearable sensors: EEG, ECG, blood pressure, body temperature
  - Hearing aids, Wellness / Fitness sensors, Baby care
- Consumer Electrics (CE)
  - Wearable audio & Video stream
  - Remote control & I/O devices: Imaging

## Consideration in BAN Channel

- Mutual interactions between body and antenna
- Distortion of directivity (Null appearance)
- Loss due to body (Absorption, impedance mismatch, distance dependent)
- Polarization rotation due to installation
- Antenna miniaturization
- SAR (Specific Absorption Rate) limitation
- Difficult to separate antenna effect from measured channel response

## Measurement Configuration

The measurements were performed in a radio anechoic chamber to avoid some effects by reflection from the surroundings. The Tx antenna was placed on around navel and the measurements were conducted at 10 Rx positions, respectively as shown in Fig. 1

Parameter	Value
Sounder	Medav channel sounder
Antenna positions	Tx : navel (fixed), Rx : 10 positions about 10,000
Number of snapshots	about 10,000
Postures	Still, walking on the spot, stand up seat down on the chair
Acquisition time	about 10 seconds
Calibration	Back to back

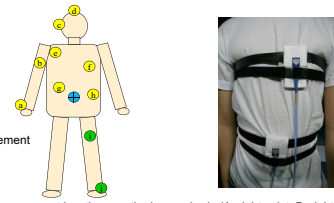


Fig. 1 Measurement locations on the human body (A: right wrist, B: right upper arm, C: left ear, D: head, E: shoulder, F: chest, G: right rib, H: left waist, I: Thigh, J: Ankle)

## Dynamic Channel Characteristics

We model the distribution of the path gain assuming quasi-static channel during the burst transmission. At first, we computed the relative path gain from the measurement data and produced cumulative distribution functions of the relative path gain of each Rx position and posture. Normal, Log-normal and Weibull distribution were used for distribution fitting. We found that the log-normal for small movement and Weibull distribution for large movement provide a characterization measure of dynamic behavior on human surface wireless propagation channel.

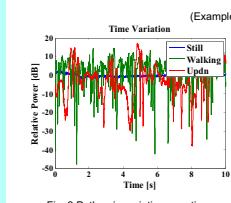


Fig. 2 Path gain variation over time

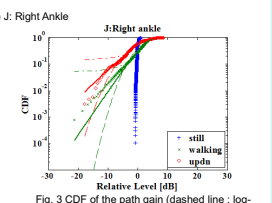


Fig. 3 CDF of the path gain (dashed line: log-normal distribution fitting and dotted line: Weibull distribution fitting)

## Best Fit Distributions

		Still	walking	updn
A	Right wrist	Normal	Weibull	Weibull
B	Right upper arm	Log-normal	Weibull	Weibull
D	Head	Weibull	Log-normal	Log-normal
E	Right ear	Normal	Log-normal	Weibull
F	Shoulder	Log-normal	Weibull	Weibull
G	Chest	Log-normal	Log-normal	Weibull
H	Right rib	Log-normal	Log-normal	Weibull
I	Left waist	Normal	Log-normal	Weibull
J	Right thigh	Log-normal	Log-normal	Weibull
K	Right ankle	Log-normal	Weibull	Weibull

# Ultra Wide Band (UWB) Delay Estimation

Marzieh DASHTI<sup>Ⓢ</sup> · Jun-ichi TAKADA<sup>Ⓢ</sup> · M ir GHORAISHI<sup>Ⓢ</sup> · Katsuyuki HANEDA<sup>\*</sup> · Ken-ichi Takizawa<sup>Ⓢ</sup>

<sup>Ⓢ</sup> Takada Laboratory, Mobile Communications Research Group, Tokyo Institute of Technology

<sup>Ⓢ</sup> The Center for Research and Development of Education Technology

<sup>\*</sup> Helsinki University of Technology

<sup>Ⓢ</sup> National Institute Information and Communications Technology

### Localization

> Basic function of a Localization System: Gathering information about the position of a mobile station and process these information to form a location estimate.

> Indoor Localization: Global positioning system(GPS) has little or no indoor coverage

> Location estimation can be implemented based on radio signal parameters:

- Received Signal Strength (RSS)
- Angle of arrival (AoA)
- Time of arrival (ToA)
- Time difference of arrival (TDoA)

> Accuracy of each location method depends on network density, radio propagation environment and algorithms.

> Different techniques can be used in different environment (indoor, urban, rural) and for different services (requirements vary)

Figure 1. Mobile localization

### ToA-Based Localization

> UWB signals have relative bandwidth larger than 20% or absolute bandwidth of more than 500MHz. This property allows extremely accurate location estimates using ToA-based techniques via UWB radios.

> ToA data fusion method is based on combining estimates of the TOA of the Transmitter node (Tx) signal when arriving at three different Receiver (Rx) nodes.

> Distance between an Tx and a Rx node is measured by finding one-way propagation time between them. This provides a circle, centered at Rx, on which Tx must lie.

> By using at least three Rx nodes, the Tx position is given by the intersection of the circles.

Figure 2. ToA Based Localization

### Threshold Based ToA Estimation

> The aim of the ToA estimator is to determine the earliest signal arrival time, or equivalently the propagation delay of the first multipath component.

> Considering the strongest path to be the first arrival path is the simplest way of achieving a ToA estimation.

> The strongest path in many cases even in line of sight (LoS) scenario is not the first arrival path.

> Several schemes have been reported for ToA estimation, among these schemes, the threshold-based ToA estimation has attracted interest due to simplicity of its hardware implementation.

> The threshold level can be selected based on the noise level or strongest path signal level.

Figure 3. Threshold based ToA estimation

### Distance Dependent threshold for UWB ToA Estimation

> In the conventional threshold selection methods, a single value is optimized as the threshold for any channel realization.

> The single value threshold is independent of Tx-Rx distance.

> We introduce a distance-dependent threshold-based method, which is postulated on the fact that power of the direct path decreases as Tx-Rx distance increases.

> The threshold value for detecting the direct path peak is a function of Tx-Rx distance.

> Setting the threshold as a function of Tx-Rx distance instead of a single value as in conventional methods, can decrease the false alarm probability.

Figure 4 Distance dependent threshold for ToA estimation